SLAC-PUB-2131
June 1978
(T/E)

NEW LIMITS ON QUARK AND LEPTON WEAK COUPLINGS*

R. Michael Barnett

Stanford Linear Accelerator Center

Stanford, California 94305

ABSTRACT

The unique determination of the weak neutral-current couplings of u and d quarks is discussed. Knowledge of these quark couplings has important implications for the determination of the electron's couplings. Recent data provide new restrictions on the charged-current couplings of quarks. The implications of these analyses for weak and electromagnetic gauge theories of quarks and leptons are examined.

Invited talk presented at the International Conference on Neutrino Physics - Neutrinos '78, Lafayette, Ind., 28 April - 2 May 1978.

---

*Research supported in part by the Department of Energy.

I. INTRODUCTION

In just a few years, enormous progress has been made in the determination of the weak couplings of both quarks and leptons. Most of this progress has occurred from analyses of processes in which neutrinos are scattered off nucleons or electrons. With the resolution of present experimental disparities, the searches for parity-violation in atomic transitions can make an important contribution. In the near future a SLAC experiment in which polarized electrons are scattered off deuterium will be reported; the measured asymmetry will further determine the electron's couplings.

In Sec. II the implications of various types of experiments on the neutral-current couplings of quarks and leptons are discussed. In Sec. III consideration is given to the role of differential and total cross-sections in finding limits on the charged-current couplings of u and d quarks to new, heavy quarks. These results are examined in the light of gauge models of the weak and electromagnetic interactions in Sec. IV.

II. NEUTRAL CURRENTS

In this section the earlier parts concern u and d quark couplings, and the latter parts concern electron couplings. All of the work described here was done together with Larry Abbott.[1]

It is assumed here that there are only V and A currents. The currents of s and c quarks are neglected. The notation used in this section has u_L, d_L, u_R and d_R (L ≡ left and R ≡ right) as the coefficients in the effective neutral-current coupling:

$$\mathscr{L}=\frac{G}{\sqrt{2}}\,\bar{\nu}\gamma_\mu(1+\gamma_5)\nu\left[u_L\,\bar{u}\gamma_\mu(1+\gamma_5)u + u_R\,\bar{u}\gamma_\mu(1-\gamma_5)u\right.$$
$$\left.+d_L\,\bar{d}\gamma_\mu(1+\gamma_5)d + d_R\,\bar{d}\gamma_\mu(1-\gamma_5)d\right] \qquad (2.1)$$

In the Weinberg-Salam (WS) model[2] with the Glashow-Iliopoulos-Maiani (GIM) mechanism[3] incorporated, u_L is equal to $\frac{1}{2} - \frac{2}{3}\sin^2\Theta_W$ with Θ_W a free parameter of the theory; u_R, d_L and d_R have similar forms.

Note that there is no assumption about the bosons carrying the neutral current, only an assumption that the effective Lagrangian 2.1 holds.

A. Neutrino-Nucleon Inclusive Scattering

The calculation of deep-inelastic neutrino scattering off nucleons ($\nu N \to \nu X$) is done using the parton model. For sake of discussion

only, let us neglect sea contributions and scaling violations (from QCD). For an isoscalar target, one finds that the neutral-current (NC) and charged-current (CC) cross-sections for neutrinos are:

$$\sigma_\nu^{NC} = \frac{G^2 mE}{\pi} \int dx\ F(x) \left[(u_L^2 + d_L^2) + \frac{1}{3}(u_R^2 + d_R^2) \right] \tag{2.2}$$

$$\sigma_\nu^{CC} = \frac{G^2 mE}{\pi} \int dx\ F(x) \left[1 \right] \tag{2.3}$$

Then the ratios for neutrinos and for antineutrinos are

$$R_\nu \equiv \frac{\sigma^{NC}}{\sigma^{CC}} = \frac{(u_L^2 + d_L^2) + \frac{1}{3}(u_R^2 + d_R^2)}{(1)} \tag{2.4}$$

$$R_{\bar{\nu}} \equiv \frac{\sigma^{NC}}{\sigma^{CC}} = \frac{\frac{1}{3}(u_L^2 + d_L^2) + (u_R^2 + d_R^2)}{\left(\frac{1}{3}\right)} \tag{2.5}$$

Therefore, one can determine the values of $(u_L^2 + d_L^2)$ and of $(u_R^2 + d_R^2)$, which are the radii in the left (L) and right (R) coupling planes. The available data[4] are shown in Fig. 1 along with the predictions of the WS model.

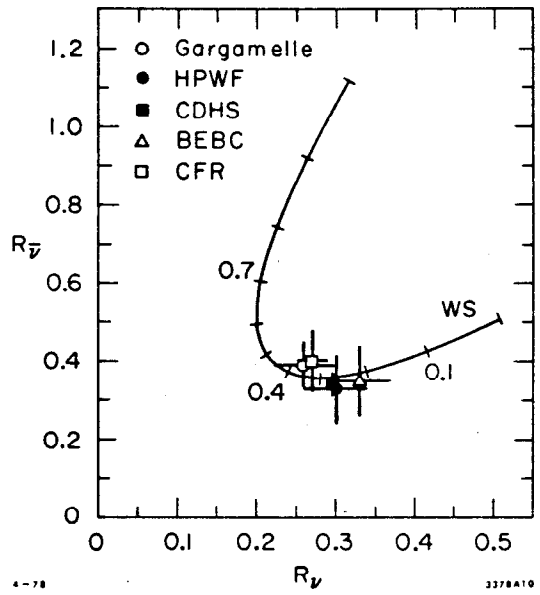

Fig. 1. The ratio of neutral to charged-current deep-inelastic scattering cross-sections for antineutrinos versus that ratio for neutrinos. The curve shows the predictions of the WS model as a function of $\sin^2\theta_W$ (each tick mark indicates a tenth value of $\sin^2\theta_W$). The data are from Ref. 4.

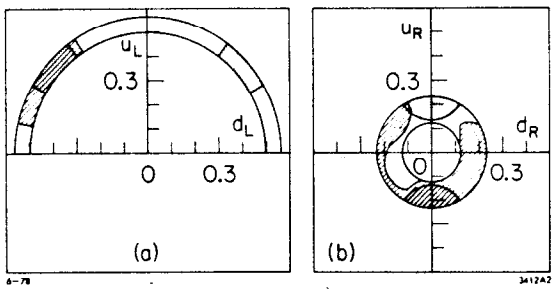

Fig. 2. The left (a) and right (b) coupling planes. The annular regions are allowed by deep-inelastic data. The region shaded with lines is allowed by elastic and exclusive-pion data. The regions shaded with dots are allowed by the inclusive-pion data.

Using the data[4] of the CERN-Dortmund-Heidelberg-Saclay (CDHS) group ($R_\nu = 0.295 \pm 0.01$ and $R_{\bar{\nu}} = 0.34 \pm 0.03$), the values of the radii in the L and R planes allowed at the 90% confidence level are shown in Fig. 2. An overall sign ambiguity among the four couplings is resolved by requiring $u_L > 0$.

B. Inclusive Production of Pions by Neutrinos

The allowed radii are well determined by deep-inelastic scattering. It remains to determine the allowed angles in the left and right planes. Let us define

$$\begin{aligned} \theta_L &\equiv \arctan\ (u_L/d_L) \\ \theta_R &\equiv \arctan\ (u_R/d_R) \end{aligned} \tag{2.6}$$

One means of determining the angles is through use of inclusive pion production ($\nu N \to \nu \pi X$). Again parton model assumptions are involved in the calculations. This analysis has been discussed by Sehgal, Hung and Scharbach.[5] It is assumed that pions produced in the current-fragmentation region (leading pions) are decay products of the struck quark. If z is defined as E_π/E_{had} (where E_{had} = [total hadron energy] = energy of the struck quark), then $D_q^\pi(z)$ describes the probability that a given pion has a fraction z of energy of the struck quark q. The calculations are similar to those for inclusive deep-inelastic scattering except that the limited specification of the final state requires that the u coupling be multiplied by $D_u^\pi(z)$ and d couplings by $D_d^\pi(z)$. Then the ratio of π^+ to π^- production for neutrinos is (neglecting sea contributions for discussion only):

$$\left(\frac{N_\pi^+}{N_\pi^-}\right) = \frac{\left(u_L^2 + \frac{1}{3}\,u_R^2\right)D_u^{\pi^+} + \left(d_L^2 + \frac{1}{3}\,d_R^2\right)D_d^{\pi^+}}{\left(u_L^2 + \frac{1}{3}\,u_R^2\right)D_u^{\pi^-} + \left(d_L^2 + \frac{1}{3}\,d_R^2\right)D_d^{\pi^-}} \tag{2.7}$$

where one requires $z > z_1$ (leading pions), $z < z_2$ (avoids resonance region) and $E_{had} > E_o$; the values of z_1, z_2, and E_o depend on the particular experiment.

There are isospin relations

$$D_u^{\pi^+} = D_d^{\pi^-} \text{ and } D_u^{\pi^-} = D_d^{\pi^+} \tag{2.8}$$

which help simplify Eq. 2.7. Furthermore, the ratio of $D_u^{\pi^+}$ to $D_u^{\pi^-}$ can be measured in ep scattering and in charged-current neutrino scattering; the relevant ratio is

$$\eta \equiv \int_{z_1}^{z_2} dz\, D_u^{\pi^+}(z) \Big/ \int_{z_1}^{z_2} dz\, D_u^{\pi^-}(z) \tag{2.9}$$

Using Eqs. 2.8 and 2.9 in Eq. 2.7 one obtains

$$\left(\frac{N_\pi^+}{N_\pi^-}\right)_\nu = \frac{\left(u_L^2 + \frac{1}{3}u_R^2\right)\eta + \left(d_L^2 + \frac{1}{3}d_R^2\right)}{\left(u_L^2 + \frac{1}{3}u_R^2\right) + \left(d_L^2 + \frac{1}{3}d_R^2\right)\eta} \tag{2.10}$$

For antineutrinos, Eq. 2.10 holds if one interchanges L and R. There are corrections to Eq. 2.10 from sea contributions and from experimental efficiencies.

Although one would prefer high energy data, the only data presently available are from Gargamelle[6] at the CERN PS. These data are $(N_\pi^+ / N_\pi^-)_\nu = 0.77 \pm 0.14$ and $(N_\pi^+ / N_\pi^-)_{\bar\nu} = 1.64 \pm 0.36$ for $0.3 < z < 0.7$ and $E_{had} > 1$ GeV. These are shown in Fig. 3 along with the predictions of the WS model.

As can be seen in Fig. 2, the pion-inclusive data (even with 90% confidence levels) place severe restrictions on the allowed angles.

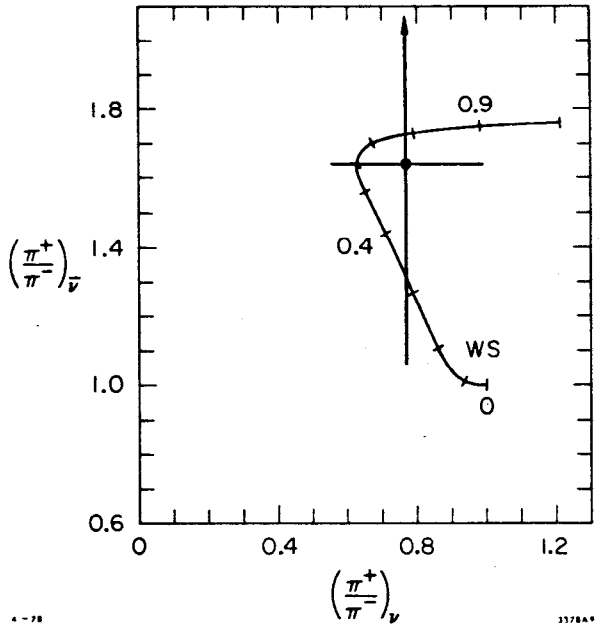

Fig. 3. The ratio of $\sigma(\bar\nu N \to \bar\nu \pi^+ X)$ to $\sigma(\bar\nu N \to \bar\nu \pi^- X)$ for antineutrinos versus that ratio for neutrinos. The curve shows the predictions of the WS model as a function of $\sin^2\Theta_W$. The data are from Ref. 6.

However, since the ratios (Eq. 2.10) are functions of the squares of the couplings, there are various sign ambiguities.

C. Elastic Neutrino-Proton Scattering

Further determination of the allowed angles along with resolution of some sign ambiguities can be obtained from analysis[1,7] of elastic neutrino-proton scattering ($\nu p \to \nu p$). Unlike the calculations of Secs. IIA and B, no parton model assumptions are needed here. The matrix element for the process is

$$\langle p' | J_\mu | p \rangle = \bar{u}(p') \left[\gamma_\mu F_1 + \frac{i\sigma_{\mu\nu} q^\nu}{2m} F_2 + \gamma_5 \gamma_\mu F_A \right] u(p) \qquad (2.11)$$

The vector form factors $[F_i(q^2)$ and $F_2(q^2)]$ are related via CVC to the electromagnetic form-factors of protons and neutrons:

$$\text{Isovector} \quad F_i = F_i^p - F_i^n \qquad (2.12)$$

$$\text{Isoscalar} \quad F_i = F_i^p + F_i^n \qquad (2.13)$$

The isovector part of the axial-vector form-factor has been measured and has the form:

$$F_A(q^2) = \frac{1.23}{(1 + Q^2/m_A^2)^2} \qquad (2.14)$$

where $m_A^2 \approx 0.79$ GeV^2 (our results are not very sensitive to variation of m_A). The isoscalar part of the axial-vector form factor is assumed to have the same Q^2 dependence; it usually makes a fairly small contribution.

The appropriate factors between these four terms are obtained using the SU(6) wavefunctions of nucleons. The data of the Harvard-Pennsylvania-Wisconsin (HPW) group[8] are $R_\nu \equiv \sigma^{NC}/\sigma^{CC} = 0.11 \pm 0.02$ and $R_{\bar{\nu}} = 0.20 \pm 0.05$ (statistical errors shown). These are shown in Fig. 4 along with the predictions of the WS model.

The resolution of the sign ambiguities remaining from the pion-inclusive data is difficult to see in Fig. 2 since correlations between the left and right planes are not evident. Since the radii in those planes are well-determined, it is useful to plot θ_L vs. θ_R (see Eq. 2.6) as in Fig. 5. The pion-inclusive data result in four allowed regions (appearing as ellipses in Fig. 5); there would be eight regions except that $d_R \approx 0$ so that 4 pairs of regions coalesce.

By "inverting" the νp elastic scattering data (with the analysis described above), one can rule out one of these four regions

Fig. 4. The ratio of neutral to charged-current elastic νp scattering cross-section for antineutrinos versus that ratio for neutrinos where $0.4<Q^2<0.9$ GeV^2. The curve shows the predictions of the WS model as a function of $\sin^2\theta_W$. The data are from Ref. 8; only statistical uncertainties are shown.

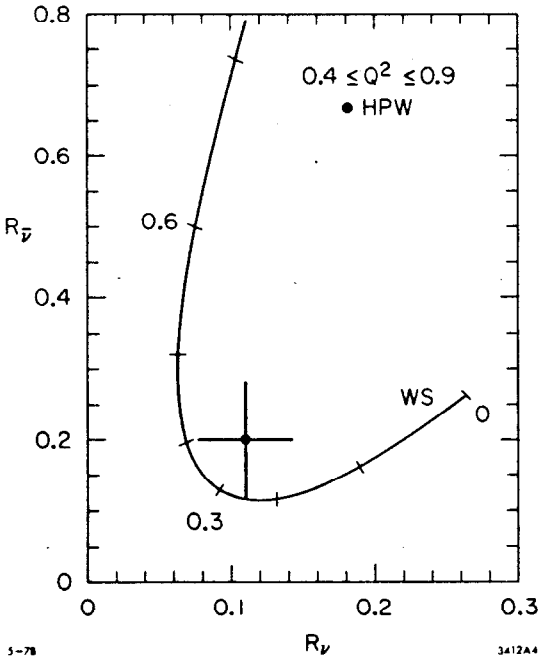

Fig. 5. The allowed angles in the coupling planes with the radii taken from Fig. 2. The area shaded with lines and enclosed by the dotted curve is allowed by elastic data. The area which is cross-hatched is allowed by elastic and exclusive-pion data. The area shaded with dots is the only region allowed by all the data.

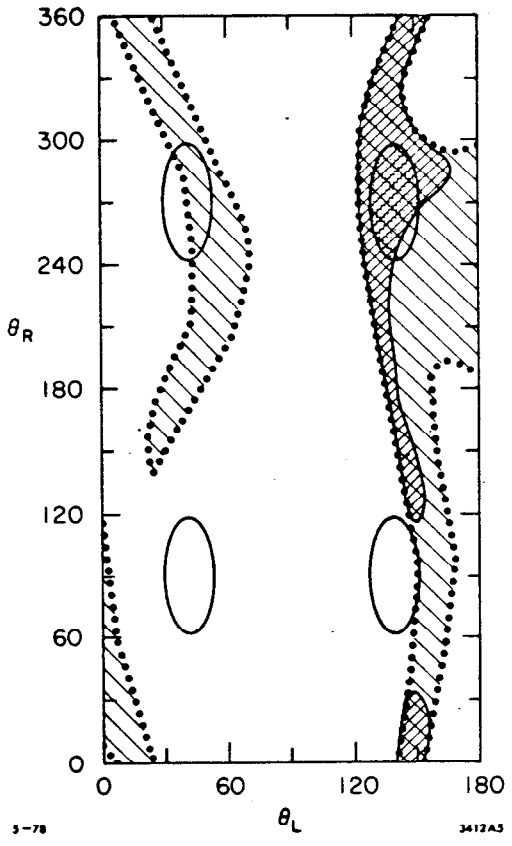

completely and can rule out substantial portions of two others. Varying portions of three regions do remain allowed. Independent of the pion-inclusive data, the elastic data severely limit the allowed regions in coupling space.

D. Production of Exclusive Pion Modes by Neutrinos

Two of the three remaining allowed regions in Fig. 5 can be ruled out by consideration of the cross-section ratios for six exclusive channels containing a pion:

$$\sigma(\nu p \to \nu p \pi^0)/\sigma_1 \tag{2.15}$$

$$\sigma(\nu n \to \nu n \pi^0)/\sigma_1 \tag{2.16}$$

$$\sigma(\nu n \to \nu p \pi^-)/\sigma_1 \tag{2.17}$$

$$\sigma(\nu p \to \nu n \pi^+)/\sigma_1 \tag{2.18}$$

$$\left[\sigma(\bar{\nu} p \to \bar{\nu} p \pi^0)+\sigma(\bar{\nu} n \to \bar{\nu} n \pi^0)\right]/\sigma_2 \tag{2.19}$$

$$\sigma(\bar{\nu} n \to \bar{\nu} p \pi^-)/\sigma_2 \tag{2.20}$$

$$\text{with } \sigma_1 \equiv \sigma(\nu n \to \mu^- p \pi^0) \tag{2.21}$$

$$\sigma_2 \equiv \sigma(\bar{\nu} p \to \mu^+ n \pi^0) \tag{2.22}$$

where recent Gargamelle data[9] were used.

To analyze the data, the detailed pion-production model developed by Adler[10] was used. This model is superior to all other pion-production models; it includes non-resonant production (an important feature), incorporates excitation of the $\Delta(1232)$ resonance, and satisfies current algebra constraints. The model gives quite good descriptions of a variety of data and is crucial for analysis of the Gargamelle data.

One begins with the Born amplitudes shown in Fig. 6 which are given in terms of the form factors F_1, F_2 and F_A (described in Sec. III C), F_π (coming from Fig. 6c) and g_r (the pion-nucleon coupling). There are two types of corrections applied.

One comes from using the current algebra relation:

$$T\left\{\partial^\mu J^5_\mu \mathcal{J}\right\} = -\delta(x_o)\left[J^5_o, \mathcal{J}\right] + \partial^\mu T\left\{J^5_\mu \mathcal{J}\right\} \tag{2.23}$$

(where T indicates time-ordered product, and $\mathcal{J}$ is the weak current of interest). Taking the Fourier transforms and then the matrix element between nucleon states for each piece of Eq. 2.23, one finds from PCAC that the left side is proportional to the

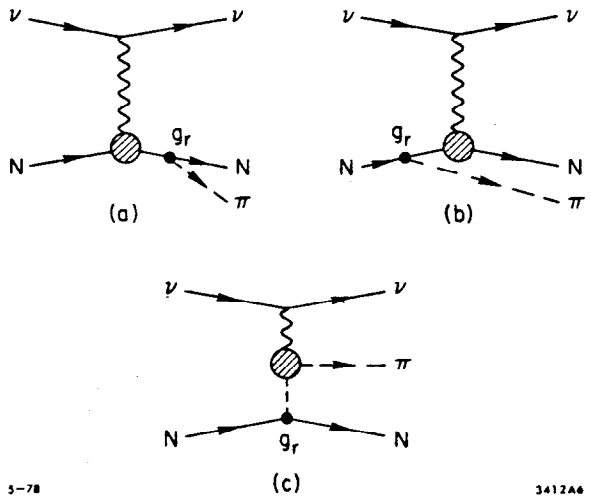

Fig. 6. The Born terms for the exclusive production of single pions, $\nu N \to \nu N \pi$.

desired matrix element $\langle N\pi | \mathcal{J}(0) | N \rangle$. The first term on the right side leads to additional form factor terms. The second term containing the J^5 current with axial-vector couplings rather than the pseudo-scalar coupling assumed for the pion, implies certain vertex corrections.

The second type of correction is for final-state interactions; the outgoing pion and nucleon can resonate. In particular for the appropriate $I=\frac{3}{2}$ terms one must account for the $\Delta(1232)$ resonance. There are the usual phase shifts ($e^{i\delta_R}$) and enhancement effects for this P_{33} resonance. It is crucial to keep the non-resonant (including $I=\frac{1}{2}$) pieces; both the analysis and the data say those pieces are significant.

To avoid other (higher mass) resonances and for consistency with the soft-pion assumptions of current algebra, it is necessary to require that the invariant mass W of the pion-nucleon system be less than 1.4 GeV. Unfortunately, the data are not available with this cut, and for modes with final-state neutrons it is, of course, quite difficult to obtain the invariant mass. However, the relevance of the cut to our conclusions is minimized because: 1) most data are below the W=1.4 GeV cut, 2) ratios of cross-sections are used, 3) application of the cut to the limited experimental mass plots available indicates a strengthening of our conclusions, and 4) the model predictions are assumed to be valid only to within 30% and the data to the 90% confidence level (this is somewhat different from the procedure followed in the first paper of Ref. 1). This fourth point is approximately equivalent to allowing any theoretical values which lie within a factor of two of the various data.

Our analysis of the six exclusive pion-production channels shows that small values of Θ_L ($\Theta_L < 90^\circ$) are totally forbidden by these data. Recall that there were four regions in Fig. 5 allowed by pion-inclusive data, and that one was ruled out by the elastic data. A second region (with $\Theta_L \approx 40^\circ$ and $\Theta_R \approx 270^\circ$ in Fig. 5) is now completely ruled out. A third region (with $\Theta_L \approx 140^\circ$ and $\Theta_R \approx 90^\circ$), which was mostly forbidden by elastic data, is not

allowed by these data. This region does appear (in Fig. 5) to be close to an area allowed by exclusive-pion-production data. However, it should be emphasized that even this latter area is quite marginal and would completely disappear if model predictions were taken as valid to 20%.

What remains is a single region (with $\theta_L \approx 140^\circ$ and $\theta_R \approx 270^\circ$) which is in good agreement with all four types of neutrino experiments. This unique determination can be expressed in terms of the coupling constants so that the allowed region (see Fig. 2) is

$$u_L = 0.35 \pm 0.07 \quad u_R = -0.19 \pm 0.06$$
$$d_L = -0.40 \pm 0.07 \quad d_R = 0.0 \pm 0.11 \tag{2.24}$$

where the errors are 90% confidence levels and an overall sign convention ($u_L \geq 0$) has been assumed. The appearance of Figs. 2 and 5 is somewhat different from those in the first paper of Ref. 1 because of new data and slightly different criteria.

Discussion of the implications of these results for gauge models of quarks is given in Sec. IV. Here it suffices to say that these results are consistent with the predictions of the WS model, but not with those of most other models.

E. Determination of the Electron's Couplings

While almost every home in America may have an electron accelerator, the weak neutral-current couplings of the electron appear to be somewhat elusive. There are two types of experiments which have been completed which should provide information on this subject. Unfortunately, in each case, conflicting results have been reported by various experimental groups, so that no conclusions can be drawn yet.

If one assumes that there is only one Z^0 boson which can carry weak neutral-currents, then our unique determination of quark couplings (shown above) allows for direct determination of electron couplings from experiments which involve weak interactions between electrons and nucleons (although one must still await resolution of experimental conflicts).

One type of experiment involves the search for parity-violation in atomic transitions in Bismuth. The details of these experiments have been given elsewhere.[11] Clearly such effects are proportional to the VA interference terms, and, in the case of Bismuth, the $(V_{hadron}\, A_{electron})$ term is completely dominant. The optical rotation ρ which is measured is then proportional to this term, i.e.- $\rho = KQ_w$, where K is a constant and (with the one Z^0 assumption)

$$Q_w = -4\, V_{had}\, g_A \tag{2.25}$$

If one defines e_L and e_R as the coefficients in the effective neutral-current coupling:

$$\mathcal{L} \propto \frac{G}{\sqrt{2}} \left[e_L \bar{e} \gamma_\mu (1+\gamma_5) e + e_R \bar{e} \gamma_\mu (1-\gamma_5) e \right] \tag{2.26}$$

then

$$\begin{aligned} g_A &\equiv (e_L - e_R) \\ g_V &\equiv (e_L + e_R) \end{aligned} \tag{2.27}$$

and

$$\begin{aligned} V_{had} = {} & (2u_L + d_L + 2u_R + d_R)Z \\ & + (u_L + 2d_L + u_R + 2d_R)N \end{aligned} \tag{2.28}$$

where Z and N are the numbers of protons and neutrons (for Bismuth, Z=83 and N=126).

Although there is some question[12] about the atomic and nuclear calculations of K (where $\rho = K Q_w$), present theoretical estimates for K are such that the optical rotations ρ for the two transitions that have been measured are

$$\rho \approx 1.1 \times 10^{-9} \, Q_w \text{ radians (for 8757 Å)} \tag{2.29}$$

$$\rho \approx 1.5 \times 10^{-9} \, Q_w \text{ radians (for 6476 Å)} \tag{2.30}$$

Two experiments report results consistent with zero: the Washington group[12] reports $\rho = (-0.5 \pm 1.7) \times 10^{-8}$ for the 8757 Å transition while the Oxford group[13] reports $\rho = (+2.7 \pm 4.7) \times 10^{-8}$ for the 6476 Å transition. By contrast the Novosibirsk experiment[14] found $\rho = (-21. \pm 6.) \times 10^{-8}$ for the 6476 Å transition.

Assuming that there exists only one Z^o boson, then the quark couplings Eq. 2.24 imply that $g_A \approx 0 \pm 0.06$ for the first two experiments, and $g_A \approx -0.4 \pm 0.17$ for the Novosibirsk experiment.

The WS model predicts $g_A = -0.5$ (independent of $\sin^2\theta_W$); if the electron had a right-handed coupling $(N_e \, e^-)_R$ in addition to the usual coupling $(\nu_e \, e^-)_R$ in an otherwise unmodified WS model, then $g_A = 0$.

The other type of experiment for which results have been reported involves νe elastic scattering (with $\nu_\mu e$, $\bar{\nu}_\mu e$ and $\bar{\nu}_e e$ measured by various groups). The cross-sections for $\nu_\mu e$ and $\bar{\nu}_\mu e$ scattering are no Z^o assumption is involved here):

$$\frac{d\sigma^{\nu,\bar{\nu}}}{dE_e} = \frac{G \, m_e}{2\pi} \left[(g_V \pm g_A)^2 + (g_V \mp g_A)^2 \left(1 - \frac{E_e}{E_\nu}\right)^2 + (g_A^2 - g_V^2) \frac{m_e E_e}{E_\nu^2} \right] \tag{2.31}$$

where the bottom signs are for antineutrinos. For $\bar{\nu}_e e$ elastic scattering there is an annihilation term (through a W^- boson), so that in Eq. 2.31 $g_V \to g_V + 1$ and $g_A \to g_A + 1$. Knowledge of these cross-sections leads to allowed regions in a g_A-g_V plot which are ellipsoidal annuli. At this time, the new data[15] from Gargamelle for $\bar{\nu}_\mu e$ scattering appear to conflict with previous measurements.[16] Those earlier measurements were completely consistent with the WS model (with $\sin^2\theta_W \approx 0.25$) while the new measurement is not.

Results will be reported soon for a new type of experiment involving the deep-inelastic scattering of polarized electrons off deuterium and hydrogen targets. In this experiment one measures the asymmetry between the cross-sections σ_p and σ_a with electrons polarized parallel and antiparallel to the beam. If there are weak parity-violating effects, the asymmetry will be non-zero. The asymmetry is sensitive to both the $V_{had}\, A_{elec}$ and $A_{had}\, V_{elec}$ terms, and furthermore involves no difficult atomic or nuclear calculations.

For an isoscalar target (deuterium) the asymmetry (see Cahn and Gilman, Ref. 17) is, with the one Z° assumption,:

$$\frac{d\sigma_p - d\sigma_a}{d\sigma_p + d\sigma_p} = 64 \times 10^{-5}\, Q^2 \left\{ \left[\frac{2}{3}(u_L + u_R) - \frac{1}{3}(d_L + d_R) \right] g_A + \left[\frac{1-(1-y)^2}{1+(1-y)^2} \right] \left[\frac{2}{3}(u_L - u_R) - \frac{1}{3}(d_L - d_R) \right] g_V \right\} \qquad (2.32)$$

The expectations of the WS model for this asymmetry are shown in Fig. 7. Also shown are the results if the electron is given a right-handed coupling $(N_e\ e^-)_R$ in addition to its usual left-handed coupling $(\nu_e\ e^-)_L$, but assuming no other changes to the WS model are made. The present experiment will have $Q^2 = 1.4\ \text{GeV}^2$ and $y = 0.25$. A run at a higher value of y may be made in the future.

It is reasonable to expect that, within a year or two, the question of the weak neutral-current couplings of the electron will be resolved.

III. CHARGED CURRENTS

In this section several experimental inputs will be used to place limits on the couplings of the u and d quarks to heavy quarks. Some of the best limits can be obtained from examination of multi-lepton events in neutrino scattering. However, such conclusions depend on assumptions about branching ratios of quarks to modes involving leptons, and I wish to avoid such assumptions here and will not use these inputs.

There are aspects of quantum-chromodynamics (QCD) which enter into

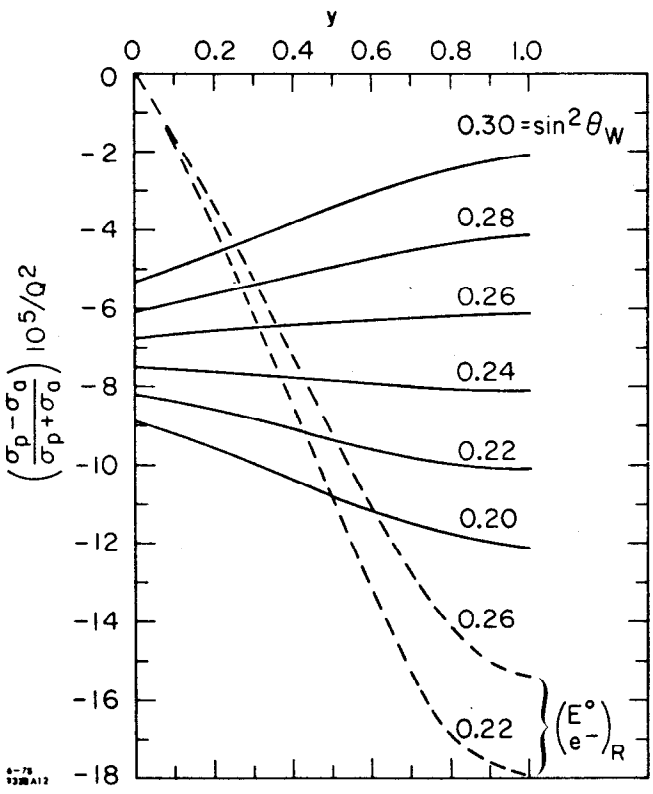

Fig. 7. The asymmetry between the cross-sections for electrons polarized parallel and antiparallel to the beam in $e^-p \to e^-X$ as a function of $y \equiv (E_e - E_{e'})/E_e$. The solid lines are the predictions of the WS model for various values of $\sin^2\theta_W$. The dashed curves are the predictions of a model in which the electron has both left and right-handed charged-current couplings (N_e is massive), but which is otherwise identical to the WS model.

the analyses of this section. The details of such calculations are given elsewhere.[18] Wherever QCD corrections are relevant in this discussion (and in all figures), they have been included.

In the notation used here g(L;ub) and g(R;ub) are defined as the coefficients (or "mixing angles") in the effective charged-current coupling:

$$\mathcal{L} = \frac{G}{\sqrt{2}} \bar{\mu}\gamma_\mu(1+\gamma_5)\nu \left[g(L;ub)\bar{b}\gamma_\mu(1+\gamma_5)u + g(R;ub)\bar{b}\gamma_\mu(1-\gamma_5)u \right] \tag{3.1}$$

where

$$g^2(L;ud) \equiv \cos^2\theta_c = 0.95. \tag{3.2}$$

In this discussion b and t are defined as heavy ($m \gtrsim 5$ GeV) quarks with charges -1/3 and 2/3, respectively.

A. Limits in the WS Model

When one has six quarks[19] in the WS model with a generalized GIM

mechanism, then the couplings are

$$\begin{pmatrix} u \\ d' \end{pmatrix}_L \quad \begin{pmatrix} c \\ s' \end{pmatrix}_L \quad \begin{pmatrix} t \\ b' \end{pmatrix}_L \tag{3.3}$$

where right-handed components are all singlets. The weak-interaction eigenstates d′, s′, b′ are not identical to the mass eigenstates d, s, b (i.e. - there is mixing).

Papers by Ellis, Gaillard, Nanopoulos and Rudaz[20] have shown that using the most general weak coupling matrix (which has four independent "mixing" angles), one can obtain limits on g(L;ub) and g(L;td). From the universality (equality) of quark and lepton couplings, one finds that

$$g^2(L;ub) < 0.003 \tag{3.4}$$

which is of course much smaller than the Cabibbo mixing (0.05).

Gaillard and Lee[21] used the $K_L - K_S$ mass difference in the context of the 4-quark WS model to estimate the charmed quark mass (prior to the ψ discovery). Using an analogous method,[20] a limit on d quark couplings to t quarks (for the 6-quark model) can be obtained; the limit is dependent on the mass of the t quark:

$$g^2(L;td) < 0.03 \quad m_t \approx 5 \text{ GeV} \tag{3.5}$$

$$g^2(L;td) < 0.01 \quad m_t \approx 15 \text{ GeV} \tag{3.6}$$

Outside of the WS model these limits are not (in general) applicable, and one must use other experimental inputs to set limits.

B. Limits on $\bar{t}d$ Couplings

Two quantities are particularly useful for determining limits on the coupling strengths of u and d quarks to new, heavy quarks. These are the total cross-section σ_{tot} and the average value of y where

$$y \equiv (E_\nu - E_\mu)/E_\nu \tag{3.7}$$

Let us consider the limit $2mEy >> m_q^2$ where m≡proton mass and m_q≡mass of the produced quark in neutrino scattering, and let us neglect QCD corrections. Then for neutrinos, $d\sigma/dy$ for right-handed couplings has a $(1-y)^2$ dependence while for left-handed couplings it has no y dependence; in σ_{tot} this leads to a factor of 1/3 for right-handed couplings relative to left-handed couplings. For antineutrino scattering it is the reverse, i.e. - $d\sigma/dy \propto (1-y)^2$ and $\sigma_{tot} \propto \frac{1}{3}$ for left-handed couplings.

The production of t quarks (or, more precisely, of hadrons containing t quarks) from valence d quarks can occur only in neutrino

scattering (not in antineutrino scattering). For $\bar{t}d_L$ couplings the resulting y dependence (in the limit $2mEy \gg m_t^2$) is the same as for the usual $\bar{u}d_L$ coupling and is therefore difficult to separate; it is better to look at σ_{tot}. For $\bar{t}d_R$ couplings, σ_{tot} has a factor of 1/3 relative to that for $\bar{u}d_L$, and testing for $\bar{t}d_R$ couplings is more difficult.

Since the relevant region is the threshold region which is $2mEy \approx m_t^2$, one must consider the implications of the parton model there.[22] The x and y dependence are no longer factorizable, and the cross-section for producing heavy quarks q (still neglecting QCD corrections) is:

$$\frac{d^2\sigma}{dxdy} = \frac{G^2 mE}{\pi} F_2(\xi) \left\{ (1-y) + \frac{x}{\xi} \left[\frac{1}{2} y^2 \pm (y - \frac{1}{2} y^2) \right] \right\} \tag{3.8}$$

where

$$\xi \equiv x + \frac{m_q^2}{2mEy} \tag{3.9}$$

and the "+" sign applies for left-handed couplings and "-" for right-handed couplings of neutrinos. For antineutrino scattering, the opposite signs apply.

Eq. 3.8 indicates that heavy quark production first becomes evident at large values of y; this is not surprising since y is proportional to the total hadron energy. Therefore, in the threshold region one expects <y> to increase, and only at higher energies will it decrease to the asymptotic value. This rise is evident in the curves of Fig. 8. As anticipated, <y> for neutrinos[23] sets no useful limits on the coupling $\bar{t}d_L$; the same is true about $\bar{t}d_R$ couplings which are not shown in Fig. 8.

More relevant are the total cross-sections. In Fig. 9 it is evi-

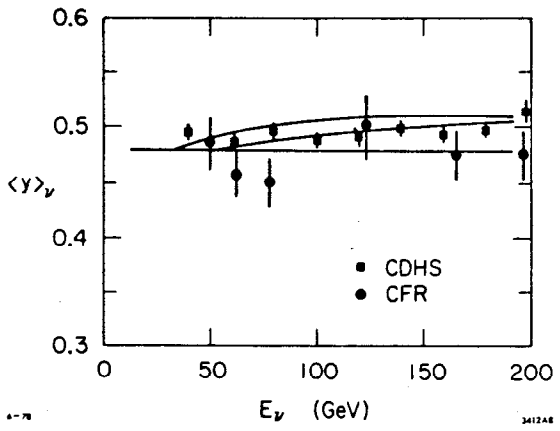

Fig. 8. The average value of y in $\nu N \to \mu^- X$ versus lab energy. The top and middle curves are the predictions for the coupling $\bar{t}d_L$ if m_t=5 and 7 GeV. The bottom curve is the standard QCD prediction without any $\bar{t}d_L$ coupling. The data are from Ref. 23.

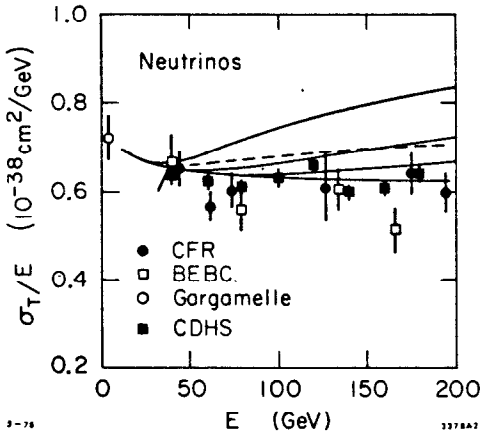

Fig. 9. The cross-section for $\nu N \to \mu^- X$ versus energy. The top three solid curves are the predictions for the coupling $\bar{t}d_L$ if m_t=5,7 and 9 GeV (from top). The dashed curve is the prediction for the coupling $\bar{t}d_R$ if m_t=5 GeV. The bottom curve is the standard QCD prediction. The data are from Ref. 24.

dent that present data[24] require that m_t>8 GeV assuming $g^2(L;td)=1.0$. Since it is not yet clear whether the quark constituting T (9.5) is a t or a b quark, it is interesting to set limits on the "mixing angles" for production of a 5 GeV quark. To avoid clutter, such curves were not included in Fig. 9. However, the second curve from the bottom is a good representation of the case when $g^2(L;td)=0.2$ (and m_t=5 GeV), and the dashed curve is a good representation of the case when $g^2(L;td)=0.4$. From these, one could estimate for $m_t \approx 5$ GeV that $g^2(L;td) \leq 0.3$ or 0.4.

For the right-handed coupling $\bar{t}d_R$ it is difficult to set any meaningful limits from these data. The dashed line in Fig. 9 shows the prediction for m_t=5 GeV and $g^2(R;td)=1.0$.

There is no evidence for the production of t quarks of either coupling although the evidence would not be visible if m_t>8 GeV.

C. Limits on $\bar{u}b$ Couplings

The production of b quarks (or, more precisely, of hadrons containing b quarks) from valence u quarks can occur only in antineutrino scattering (not in neutrino scattering). For $\bar{u}b_L$ couplings the resulting y-dependence (in the limit $2mEy >> m_b^2$) is the same $[(1-y)^2]$ as for the usual $\bar{u}d_L$ coupling (see the discussion in Sec. III B). For $\bar{u}b_R$ couplings not only is the y-dependence different (and further emphasized by threshold effects), but σ_{tot} is asymptotically 3 times larger than σ_{tot} for $\bar{u}d_L$; as a result, of the four couplings considered, this one is the easiest to detect, and strict limits can be set. For $\bar{u}b_R$ and m_b=7,9 and 11 GeV, the expected values of and the data[25,26] for $\langle y \rangle$ and σ_{tot} are shown in Figs. 10 and 11.

It has become common practice to make us of another variable B. The apparent motivation for invoking a new variable is the desire

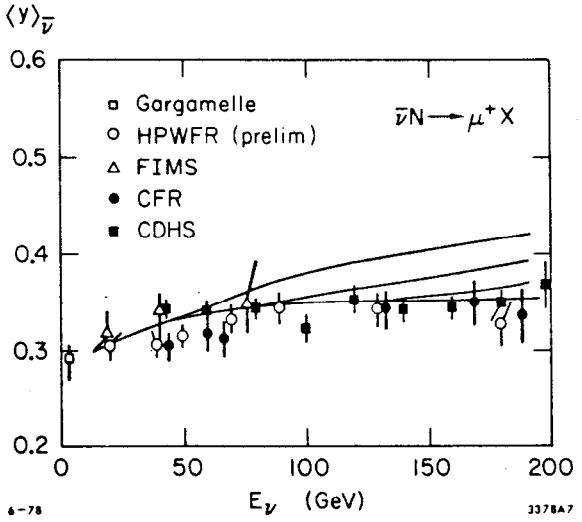

Fig. 10. The average value of y in $\bar{\nu}N \to \mu^+X$ versus lab energy. The top three curves are the predictions for the coupling $\bar{u}b_R$ if m_b=7,9 and 11 GeV (from top). The bottom curve is the standard QCD prediction with no $\bar{u}b_R$ coupling. The data are from Ref. 25.

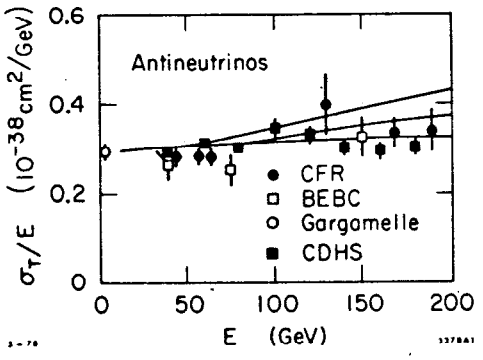

Fig. 11. The cross-section for $\bar{\nu}N \to \mu^+X$ versus energy. The top and middle curves are the predictions for the coupling $\bar{u}b_R$ if m_b=7 and 9 GeV. The bottom curve is the standard QCD prediction. The data are from Ref. 26.

to have a variable which is corrected for the different cuts and efficiencies of each experiment, so that comparisons can be made. (Of course, <y> and σ_{tot} could also be corrected.) B is defined by

$$\frac{d^2\sigma}{dxdy} = \frac{G^2 mE}{\pi} F_2(x)\left[\frac{(1\pm B)}{2} + \frac{(1\mp B)}{2}(1-y)^2\right] \qquad (3.10)$$

where

$$B = -xF_3(x)/F_2(x) \qquad (3.11)$$

and the upper (lower) signs are for neutrinos (antineutrinos). However, in QCD this form is only approximate. In fact, using σ_{tot} and <y> to obtain the values of B leads to slightly different values of B (here <y> is used).

Examination of Fig. 12 (or of Figs. 10 and 11) indicates that if $g^2(R;ub)$=1.0, then the limit $m_b \geq 11$ GeV results. If (in considera-

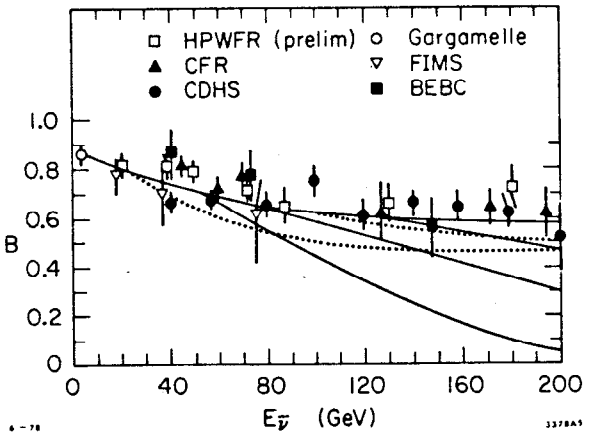

Fig. 12. The value of B (defined in text) from $\bar{\nu}N \to \mu^+X$ as a function of lab energy. The bottom three curves are the predictions for the coupling $\bar{u}b_R$ if m_b=7,9 and 11 GeV (from bottom). The two dotted curves are the predictions for the coupling $\bar{u}b_L$ if m_b=5 and 9 GeV (from bottom). The top curve is the standard QCD prediction with no $\bar{u}b$ couplings. The data are from Refs. 25 and 26.

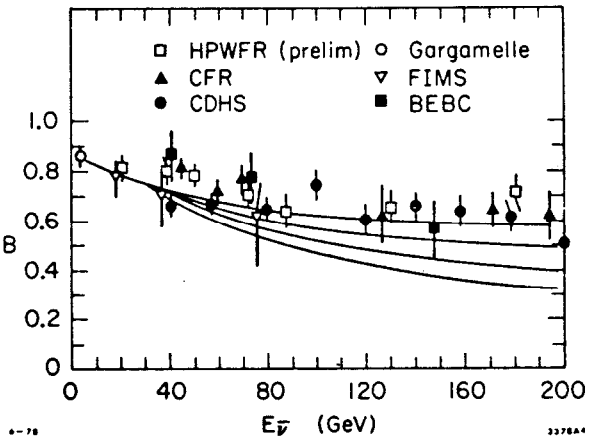

Fig. 13. The value of B (defined in text) from $\bar{\nu}N \to \mu^+X$ as a function of energy. The bottom three curves are the predictions for the couplings $\bar{u}b_R$ if m_b=5 GeV and if $g^2(R;ub)$=0.1, 0.2 and 0.3 (from top). The top curve is the standard QCD prediction. The data are from Refs. 25 and 26.

tion of T(9.5) one lets m_b=5 GeV, then from Fig. 13 one finds $g^2(R;ub) \leq 0.1$. For $\bar{u}b_L$ couplings, the limits are not strict; from Fig. 12 one has $m_b \geq 7$ GeV for $g^2(L;ub)$=1.0.

There has been question for some time on whether there was energy dependence in $\langle y \rangle$ and σ_{tot} for antineutrinos which could indicate production of b quarks through the coupling $\bar{u}b_R$. With all of these new data, it is clear that there is absolutely no evidence for production of b quarks. Nonetheless, there does appear to be some energy dependence as expected from the scaling violations which are predicted by QCD. This can be seen in Figs. 10-13 and was discussed by Fox[27] at this conference. Data concerning the separation[28] of b quark production effects from QCD effects were presented at the conference by Bobisut.[29]

D. Production of t and b Quarks

To estimate the production of particles containing heavy quarks,

one must account for the phase space suppression. Included in this suppression are the threshold effects resulting from Eqs. 3.8 and 3.9. For two neutrino fluxes of different shape, the phase space suppression is shown in Table I.

Table I - Phase Space Suppression

Quark Mass	Fermilab Quad Triplet Flux		CERN Wide Band Flux	
	All E	E>100 GeV	All E	E>100 GeV
5 GeV	0.1	0.3	0.1	0.2
10 GeV	0.006	0.03	0.001	0.01
15 GeV	10^{-4}	$6.\times10^{-4}$	10^{-5}	10^{-4}

Using these numbers and the results of Secs. III B and C, one can estimate the upper limit on the fraction of total events which could contain t or b quarks. For production through left-handed couplings, the limits for 5 GeV t quarks are 3×10^{-4} in the context of the 6-quark WS model and 7×10^{-2} in general; for 5 GeV b quarks the limits are 3×10^{-3} for the WS model and 3×10^{-2} in general.

For right-handed couplings one must recall that there is a relative factor of 3 from helicity arguments (see Sec. III B); actually in the threshold region where Eqs. 3.8 and 3.9 apply, this factor is more like 2 so that

$$\frac{\sigma^{\nu}(\bar{t}d_R)}{\sigma^{\nu}(\bar{u}d_L)} \approx \frac{1}{2} \quad \frac{\sigma^{\bar{\nu}}(\bar{u}b_R)}{\sigma^{\bar{\nu}}(\bar{u}d_L)} \approx 2 \tag{3.12}$$

Then the upper limit on the fraction of total events which contain 5 GeV t quarks produced through a right-handed coupling is 4×10^{-2} while the limit for 5 GeV b quarks produced via $\bar{u}b_R$ is 2×10^{-2}.

As stated at the beginning of this section, it is possible to obtain better limits on t and b quark production from multi-lepton events in neutrino scattering, but one must invoke assumptions about the branching ratios of these quarks to modes containing leptons.

IV. IMPLICATIONS FOR GAUGE MODELS

One of the important questions considered is whether in the context of $SU(2) \times U(1)$ models there is any evidence for right-handed charged-currents. Both the neutral-current and the charged-current results are relevant to this question, and in both cases they indicate that there are no right-handed charged-currents for u or d quarks in $SU(2) \times U(1)$ models.

To see that the neutral-current couplings rule out such right-handed

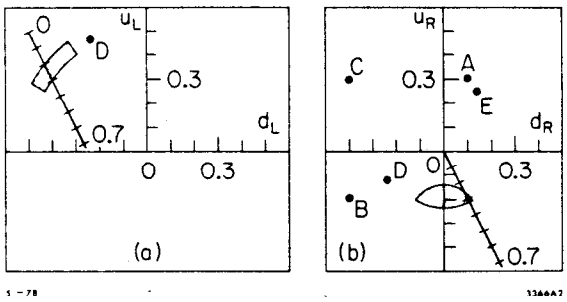

Fig. 14. Various gauge models compared with the allowed coupling constant region. The lines mark the WS model for values of $\sin^2\theta_W$ from 0.0 to 0.7. The points labeled A-E are the predictions of various models discussed in the text. For A,B,C and E u_L and d_L lie with the shaded region.

couplings, consider Fig. 14 which shows the allowed regions from Fig. 2. All $SU(2) \times U(1)$ models with the left-handed coupling doublet $\bar{u}d_L$ have values in the left-coupling plane (Fig. 14a) which are indicated by the line with tick marks. These models have $\sin^2\theta_W$ as a free parameter so that the position on the line (i.e.- the value of $\sin^2\theta_W$) is determined solely from the data. Clearly from Fig. 14a the allowed value of $\sin^2\theta_W$ is between 0.2 and 0.3.

Now looking at the right coupling plane, Fig. 14b, one sees that for the WS model the values of $\sin^2\theta_W = 0.2 - 0.3$ are also allowed there. The overall magnitude of these neutral-current couplings was dependent on the mass ratio of $m(Z^o)/m(W^\pm)$ which is predicted by the WS model[2] with the minimal Higgs boson structure (one or more doublets) to be:

$$m_{Z^o} = m_{W^\pm} / \cos\theta_W \qquad (4.1)$$

If this mass ratio were not as predicted, then the model would be ruled out (for example, one might find that $\sin^2\theta_W = 0.1$ was required by the left-coupling plane, Fig. 14a, but $\sin^2\theta_W = 0.4$ by the right-coupling plane, Fig. 14b). The success of these predictions of the WS model is remarkable.

For other $SU(2) \times U(1)$ models, if one chooses $\sin^2\theta = 0.3$ from the left-coupling-plane, then the resulting points in the right plane are determined. Shown in Fig. 14b are the points for the cases where the models have the right-handed doublets $\bar{u}b_R$ (labeled A),[30] $\bar{t}d_R$ (B)[31] and both $\bar{u}b_R$ and $\bar{t}d_R$ (C). The latter model (C)[32] has been called the "vector" model. As can be seen, these models are ruled out by the data. Varying the ratio $m(Z^o)/m(W^\pm)$ moves the points toward or away from the origin, but these models still cannot survive. There are other $SU(2) \times U(1)$ models[33] involving $-\frac{4}{3}$ and 5/3 charged quarks, and these are also ruled out.

The applicability of these results is <u>not</u> limited to $SU(2) \times U(1)$ models. For example, there are two $SU(3) \times U(1)$ models which are ruled out by these data. One[34] (labeled D in Fig. 14b) has the u quark in a right-handed singlet and the other[35] (E) has the u

quark in a right-handed triplet (for this latter case the parameters of the model were chosen to place u_L and d_L in the allowed region in Fig. 14a).

These results also apply to the $SU(2)_L \times SU(2)_R \times U(1)$ model.[36] Since that model can be chosen to have the same values of u_L, d_L, u_R and d_R as the WS model, it is allowed by the analysis of quark couplings. In fact Georgi and Weinberg[37] have generalized this conclusion by showing that at zero-momentum-transfer, the neutral-current interactions of neutrinos in an $SU(2) \times G \times U(1)$ gauge theory are the same as in the corresponding $SU(2) \times U(1)$ theory if neutrinos are neutral under G.

The $SU(2)_L \times SU(2)_R \times U(1)$ gauge model has been chosen to give zero parity-violation while still reproducing all of the neutrino cross-sections (including νe scattering) of the WS model. Therefore, the best means of distinguishing it from the WS model comes in the atomic parity-violation experiments (described in Sec. II) and from the polarized electron-proton scattering experiment. While there are discrepancies between the atomic experiments, the question of weak parity-violation could be settled by the polarized electron experiment in the very near future.

The neutral-current couplings of quarks are now known, and within a year or two those of the electron should be known. We are then faced with completing the theory of quarks and leptons; we need, for example, to understand the masses and mixing angles of fermions. Perhaps, these problems must be addressed by finding the grand unification of the fundamental interactions, or perhaps, progress toward this unification can only be made by solving these smaller problems one by one and learning more at each step.

ACKNOWLEDGMENTS

Much of the work described here was completed with L. Abbott. I have benefitted from discussions with S. Adler, J. Bjorken, F. Bobisut, F. Gilman, W. Kozanecki, A. Mann, J. Marriner, F. Martin, C. Matteuzzi, E. Monsay, F. Nezrick, Y.-J. Ng, E. Paschos, B. Roe, J. Strait, L. Sulak, H. Wahl and S. Weinberg. I would like to thank the Fermilab Theory group for their hospitality.

REFERENCES

1. L.F. Abbott and R.M. Barnett, Phys. Rev. Lett. 40, 1303 (1978) and SLAC-PUB (in preparation).
2. S. Weinberg, Phys. Rev. Lett. 19, 1264 (1967); A. Salam, in Elementary Particle Physics: Relativistic Groups and Analyticity, edited by N. Svartholm (Almquist and Wiksell, Stockholm, 1968), p. 367.
3. S.L. Glashow, J. Iliopoulos and L. Maiani, Phys. Rev. D2, 1285 (1970).
4. M. Holder et al. (CDHS), Phys. Lett. 72B, 254 (1977); J. Blietschau et al. (Gargamelle), Nucl. Phys. B118, 218 (1977); A. Benvenuti et al. (HPWF), Phys. Rev. Lett. 37, 1039 (1976); P. Wanderer et al. (HPWF), Phys. Rev. D17, 1679 (1978); F.S. Merritt et al. (CF), Phys. Rev. D17, 2199 (1978); K. Schultze (BEBC), in Proc. 1977 Int. Symp. on Lepton and Photon Interactions at High Energies, edited by F. Gutbrod (DESY, Hamburg, 1977) p. 359.
5. L.M. Sehgal, Phys. Lett. 71B, 99 (1977); P.Q. Hung, Phys. Lett. 69B, 216 (1977); P. Scharbach, Nucl. Phys. B82, 155 (1974); and Ref. 1.
6. H. Kluttig et al., Phys. Lett. 71B, 446 (1977).
7. Analyses of elastic scattering have been done by S. Weinberg, Phys. Rev. D5, 1412 (1972); M. Barnett, Phys. Rev. D14, 2990 (1976); C.H. Albright et al., Phys. Rev. D14, 1780 (1976); V. Barger and D.V. Nanopoulos, Nucl. Phys. B124, 426 (1977); D.P. Sidhu, Phys. Rev. D14, 2235 (1976); F. Martin, Nucl. Phys. B104, 111 (1976); P.Q. Hung and J.J. Sakurai, Phys. Lett. 72B, 208 (1977); P. Langacker and D.P. Sidhu, Phys. Lett. 74B, 233 (1978); G. Ecker, Phys. Lett. 72B, 450 (1978).
8. L. Sulak, Harvard report, to appear in the Proceedings of the Neutrinos-78 Conference, Purdue University, April 28-May 2, 1978; J.B. Strait and W. Kozanecki, Harvard University Ph.D. theses (1978); D. Cline et al., Phys. Rev. Lett. 37, 252 and 648 (1976); see also W. Lee et al., Phys. Rev. Lett. 37, 186 (1976); M. Pohl et al., Phys. Lett. 72B, 489 (1978).
9. W. Krenz et al., report no. CERN/EP/PHYS 77-50 (1977); O. Erriques et al., Phys. Lett. 73B, 350 (1978); see also S.J. Barish et al., Phys. Rev. Lett. 33, 448 (1974); W. Lee et al., Phys. Rev. Lett. 38, 202 (1977).
10. S.L. Adler, Ann. Phys. 50, 189 (1968), and Phys. Rev. D12, 2644 (1975); S.L. Adler et al., Phys. Rev. D12, 3501 (1975) and Phys. Rev. D13, 1216 (1976); see also E.H. Monsay, Argonne report ANL-HEP-PR-78-08 (1978); G. Ecker in Ref. 7; and Ref. 1.
11. P.E.G. Baird et al., Nature 264, 528 (1976).
12. N. Fortson, to appear in the Proceedings of the Neutrinos-78 Conference, Purdue University, April 28-May 2, 1978; E. Henley, ibid.; W.J. Marciano and A.I. Sanda, Rockefeller reports nos. COO-2232B-142 and 153 (1978); G. Feinberg, Columbia report no. CU-TP-111, to appear in the Proceedings of the Ben Lee Memorial

Int. Conf., Batavia, Illinois, Oct. 20-22, 1977.
13. P.G.H. Sandars, in Proc. 1977 Int. Symp. on Lepton and Photon Interactions at High Energies, edited by F. Gutbrod (DESY, Hamburg, 1977) p. 599.
14. L.M. Barkov and M.S. Zolotorev, Pisma Zh. Eksp. Teor. Fiz. (JETP Lett.) 26, 379 (1978).
15. P. Alibran et al., report no. CERN/EP/PHYS 78-6 (1978).
16. F.J. Hasert et al., Phys. Lett. 46B, 121 (1973); J. Blietschau et al., Nucl. Phys. B114, 189 (1976); F. Reines et al., Phys. Rev. Lett. 37, 315 (1976); M. Baldo-Ceolin, to appear in the Proceedings of the Neutrinos-78 Conference, Purdue University, April 28-May 2, 1978.
17. R.N. Cahn and F.J. Gilman, Phys. Rev. D17, 1313 (1978) and references therein.
18. See G. Fox, to appear in the Proceedings of the Neutrinos-78 Conference, Purdue University, April 28-May 2, 1978; G. Altarelli et al., Phys. Lett. 63B, 183 (1976); M. Barnett et al., Phys. Rev. Lett. 37, 1313 (1976); J. Kaplan and F. Martin, Nucl. Phys. B115, 333 (1976); V.I. Zakharov, in Proc. XVIII Int. Conf. on High Energy Physics, Tbilisi, July 1976, edited by N.N. Bogoliubov et al. (JINR, Dubna, 1977), Vol. II, p. B69; A.J. Buras, Nucl. Phys. B125 (1977).
19. M. Kobayashi and K. Maskawa, Prog. Theor. Phys. 49, 652 (1973).
20. J. Ellis et al., Nucl. Phys. B131, 285 (1977); J. Ellis et al., Nucl. Phys. B109, 213 (1976); see also T. Appelquist et al., Ann. Rev. Nucl. Sci. 28 (1978).
21. M.K. Gaillard and B.W. Lee, Phys. Rev. D10, 897 (1974).
22. M. Barnett, Phys. Rev. Lett. 36, 1163 (1976) and Phys. Rev. D14, 70 (1976); H. Georgi and H.D. Politzer, Phys. Rev. Lett. 36, 1281 (1976); E. Derman, Nucl. Phys. B110, 40 (1976); S. Pakvasa et al., Nucl. Phys. B104, 469 (1976).
23. B.C. Barish et al. (CFR), Phys. Rev. Lett. 40, 1414 (1978); H. Wahl et al. (CDHS), to appear in the Proceedings of the Neutrinos-78 Conference, Purdue University, April 28-May 2, 1978.
24. B.C. Barish et al. (CFR), Phys. Rev. Lett. 39, 1595 (1977); P.C. Bosetti et al. (BEBC and Gargamelle), Phys. Lett. 70B, 273 (1977); H. Wahl et al. (CDHS), see Ref. 23.
25. J.P. Berge et al. (FIMS), Phys. Rev. Lett. 39, 382 (1977); B.C. Barish et al. (CFR), Phys. Rev. Lett. 40, 1414 (1978); P.C. Bosetti et al., Phys. Lett. 70B, 273 (1977), the Gargamelle point was calculated from the value of B quoted in this paper; H. Wahl et al. (CDHS), see Ref. 23; F. Bobisut et al. (HPWFR), to appear in the Proceedings of the Neutrinos-78 Conference, Purdue University, April 28-May 2, 1978.
26. B.C. Barish et al. (CFR), Phys. Rev. Lett. 39, 1595 (1977); P.C. Bosetti et al. (BEBC and Gargamelle), Phys. Lett. 70B, 273 (1977); H. Wahl et al. (CDHS), see Ref. 23.
27. G. Fox, to appear in the Proceedings of the Neutrinos-78 Conference, Purdue University, April 28-May 2, 1978.

28. R.M. Barnett and F. Martin, Phys. Rev. D16, 2765 (1977).
29. F. Bobisut, to appear in the Proceedings of the Neutrinos-78 Conference, Purdue University, April 28-May 2, 1978.
30. R.M. Barnett, Phys. Rev. Lett. 34, 41 (1975), Phys. Rev. D11, 3246 (1975); P. Fayet, Nucl. Phys. B78, 14 (1974); F. Gürsey and P. Sikivie, Phys. Rev. Lett. 36, 775 (1976); P. Ramond, Nucl. Phys. B110, 214 (1976).
31. R.M. Barnett, Phys. Rev. D13, 671 (1976).
32. A. De Rújula et al., Phys. Rev. D12, 3589 (1975); F.A. Wilczek et al., Phys. Rev. D12, 2768 (1975); H. Fritzch et al., Phys. Lett. 59B, 256 (1975); S. Pakvasa et al., Phys. Rev. Lett. 35, 702 (1975).
33. R.M. Barnett, Phys. Rev. D15, 675 (1977).
34. B.W. Lee and S. Weinberg, Phys. Rev. Lett. 38, 1237 (1977); B.W. Lee and R.E. Shrock, Phys. Rev. D17, 2410 (1978); G. Segre and J. Weyers, Phys. Lett. 65B, 243 (1976).
35. R.M. Barnett and L.N. Chang, Phys. Lett. 72B, 233 (1977); R.M. Barnett et al., Phys. Rev. D17, 2266 (1978); P. Langacker and G. Segre, Phys. Rev. Lett. 39, 259 (1977).
36. J. Pati and A. Salam, Phys. Rev. D10, 275 (1974); H. Fritzsch and P. Minkowski, Nucl. Phys. B103, 61 (1976); R.N. Mohapatra and D.P. Sidhu, Phys. Rev. Lett. 38, 667 (1977); A. De Rújula, H. Georgi and S.L. Glashow, Annals Phys. 109, 242 and 258 (1977).
37. H. Georgi and S. Weinberg, Phys. Rev. D17, 275 (1978); R. Gatto and F. Strocchi, Geneva report (1978).